

Article

A Compact 2.4 GHz L-Shaped Microstrip Patch Antenna for ISM-Band Internet of Things (IoT) Applications

Muhammad Fitra Zambak ^{1,*}, Samir Salem Al-Bawri ², Muzammil Jusoh ³, Ali Hanafiah Rambe ⁴, Hamsakutty Vettikalladi ⁵, Ali M. Albishi ⁵ and Mohamed Himdi ⁶

¹ Faculty of Electrical Engineering, Universitas Muhammadiyah Sumatera Utara, Kota Medan 20238, Indonesia

² Space Science Centre, Climate Change Institute, Universiti Kebangsaan Malaysia, Bangi 43600, Malaysia; s.albawri@gmail.com

³ Advanced Communication Engineering (ACE), Centre of Excellence, Faculty of Electronic Engineering Technology, Universiti Malaysia Perlis, Kangar 01000, Malaysia; muzammil@unimap.edu.my

⁴ Department of Electrical Engineering, Universitas Sumatera Utara, Medan 20155, Indonesia; ali3@usu.ac.id

⁵ Electrical Engineering Department, College of Engineering, King Saud University, Riyadh 11421, Saudi Arabia; hvettikalladi@ksu.edu.sa (H.V.); aalbishi@ksu.edu.sa (A.M.A.)

⁶ Institut d'Electronique et des Technologies du numéRique (IETR), University of Rennes, 35042 Renne, France; mohamed.himdi@univ-rennes1.fr

* Correspondence: mhdfitra@umsu.ac.id

Abstract: Wireless communication technology integration is necessary for Internet of Things (IoT)-based applications to make their data easily accessible. This study proposes a new, portable L-shaped microstrip patch antenna with enhanced gain for IoT 2.4 GHz Industrial, Scientific, and Medical (ISM) applications. The overall dimensions of the antenna are $28\text{ mm} \times 21\text{ mm} \times 1.6\text{ mm}$ ($0.22\lambda_0 \times 0.17\lambda_0 \times 0.013\lambda_0$, with respect to the lowest frequency). The antenna design is simply comprised of an L-shape strip line, with a full ground applied in the back side and integrated with a tiny rectangular slot. According to investigations, the developed antenna is more efficient and has a greater gain than conventional antennas. The flexibility of the antenna's matching impedance and performance are investigated through several parametric simulations. Results indicate that the gain and efficiency can be enhanced through modifying the rectangular back slot in conjunction with fine-tuning the front L-shaped patch. The finalized antenna operates at 2.4 GHz with a 98% radiation efficiency and peak gains of 2.09 dBi (measured) and 1.95 dBi (simulated). The performance of the simulation and measurement are found to be in good agreement. Based on the performance that was achieved, the developed L-shaped antenna can be used in a variety of 2.4 GHz ISM bands and IoT application environments, especially for indoor localization estimation scenarios, such as smart offices and houses, and fourth-generation (4G) wireless communications applications due to its small size and high fractional bandwidth.

Keywords: Internet of Things; antenna; gain; bandwidth



Citation: Zambak, M.F.; Al-Bawri, S.S.; Jusoh, M.; Rambe, A.H.; Vettikalladi, H.; Albishi, A.M.; Himdi, M. A Compact 2.4 GHz L-Shaped Microstrip Patch Antenna for ISM-Band Internet of Things (IoT) Applications. *Electronics* **2023**, *12*, 2149. <https://doi.org/10.3390/electronics12092149>

Academic Editors: Nikolay Todorov
Atanasov, Maria Seimeni-Tsumani
and Hussain Al-Rizzo

Received: 23 March 2023

Revised: 2 May 2023

Accepted: 3 May 2023

Published: 8 May 2023



Copyright: © 2023 by the authors. Licensee MDPI, Basel, Switzerland. This article is an open access article distributed under the terms and conditions of the Creative Commons Attribution (CC BY) license (<https://creativecommons.org/licenses/by/4.0/>).

1. Introduction

The idea of the Internet of Things (IoT) has now been integrated into the Internet. It is a rapidly expanding global network of linked things that supports several input–output devices, sensors, and actuators using a common communication protocol. The effectiveness of IoT application operation and device internet connectivity are both enhanced using wireless sensor technologies [1]. With the rapid advancement of IoT technologies, ever- more applications are being found in a variety of fields, such as agriculture, tracking, security, smart cities, smart homes, etc. The antenna is one of the key components of wireless communication sensor technology that is moving into the future. Over the past few years, small and readily integrated antenna design drew a lot of attention due to the enhanced potential for using multi-frequency and multi-function antenna in communication technologies [2].

The unlicensed 2.4 GHz band used for industrial, scientific, and medical purposes transmits the combined communication data at a high frequency band. For IoT applications, the applications of a transparent loop antenna that allows deployment at various locations are also shown [3]. In [4], a planar multiple-input and multiple-output (MIMO) antenna for IoT applications was created. In [5], a loop antenna for biotelemetry Internet of Things applications was developed. A leaky-wave antenna with a fractional bandwidth of 136.5% was created in [6] for scanning applications of passive radar systems. This antenna can function with Bluetooth Low Energy (BLE), Global System for Mobile Communication 900° (GSM 900), and GSM 1800 [7]; a planar antenna with an omnidirectional radiation pattern and a fractional bandwidth of 143.66% was designed for use in Global Positioning System (GPS), Bluetooth, and Wireless Fidelity (WiFi) applications. Therefore, the primary factors that must be considered when constructing microstrip patch antennas operating in the 2.4 GHz band are radiation and total efficiencies, bandwidth (BW), radiation pattern, gain, etc. [8–10].

The wireless communication sector requires tiny, lightweight antennas with affordable fabrication [11]. As it is designed to achieve low profile reduction via implanting wire construct on a dielectric substrate, a miniaturized meander-shaped antenna is a viable option in this situation because the space available for its installation is constrained [12]. An antenna with a smaller size and fixed frequency operation was presented as a compact meandering slotted microstrip antenna [13]. Additionally, low bandwidth and low gain antennas present another difficulty for communication systems. Researchers have put forth a variety of methods for improving gain, BW and efficiency, with acceptable radiation characteristics utilizing several antennas with complicated shapes. The single frequency and small bandwidth of a microstrip antenna are two significant drawbacks. To address this problem, a tuning stub resembling a fork is attached to the microstrip slotted antenna [14]. On a 1.6 mm thick FR-4 substrate, a capacitive load (C-load) was applied to increase peak gain with a fractional BW of 7.23% and improve impedance matching, which represents a distinguished performance enhancement approach [15]. To increase the fractional bandwidth, embedded metamaterials were also used [16,17]. However, applying a parasitic patch to the antenna is a useful technique for increasing the BW and gain. The bandwidth and gain are increased by approximately 3.3 dB [18] when the parasitic patch is situated close to the feed patch. Mobile phones for 2.4 GHz have parasitic patches installed with an inverted F-antenna, and the impedance bandwidth is 90 MHz [19]. Using a parasitic element, which acts as a director in the low working range between 1.6 and 3.45 GHz, impedance matching was enhanced [20]. The circular disc monopole antenna was also given shaped ground in order to match its 50-ohm impedance [21]. When parasitic elements are applied to the microstrip antenna at frequencies of 2.99–3.10 GHz and 2.1–11.1 GHz, respectively, the impedance bandwidth likewise increases from 4.3% to 6% and 136% [22,23].

For the designing of compact antennas for 2.4 GHz ISM band applications, fractal antennas are one of best available techniques, as explained in [24,25]. The use of truncated corners is another well-studied technique to achieve compact antenna for microwave, as proposed in [26,27]. The open-ended stub loading technique is also widely studied, as explained in [28,29]. To obtain a satisfactory impedance fractional bandwidth of 2.4 GHz, a variety of different-shaped antennas of various sizes were proposed and measured [24–27]. For biotelemetry in biomedical investigative systems, a small, strong, and flexible body-worn antenna was presented in [30]. In order to ensure that the antenna is of the ideal size and works at a lower frequency band of interest, the fractal-based design lengthened the current flow. WMTS and ISM bands are simultaneously covered using the antenna's dual-band operation (1.38–1.8 GHz and 2.25–4.88 GHz). However, [31] presents a dual-band antenna for on- and off-body communications in the ISM frequencies bands of 2.45 GHz and 5.8 GHz, with silver material combined onto a stretchable polydimethylsiloxane (PDMS) substrate, which is more useful for wearable applications. In [32], a compact antenna-based PDMS with an overall size of $14 \times 33 \text{ mm}^2$ was introduced with a 15% broadband offering

and centered at 2.45 GHz. In contrast, a conformal antenna with electronic tuning capability was presented in [33]; it involves a 40 mm bending radius using a PDMS substrate, with 64% being the achieved efficiency in the broadside mode.

This paper reports a well-modified L-shaped compact antenna for 2.4 GHz ISM band IoT applications. The simulation was conducted using the Computer Simulation Technology (CST) Microwave Studio simulator. For experimental measurements, the antenna was constructed on a Rogers 5880 printed circuit board. A straightforward L-shaped strip line was attached to the feed SMA connector in this design, and integrated with an etching slot built on the backside to obtain sufficient gain and bandwidth. It is demonstrated that a ground shape can provide the gain at a constant value while improving both bandwidth and efficiency results. Additionally, an experiment to assess the performance of the antenna is provided, and the findings show that the results are in good agreement with the simulation.

2. Antenna Design

The proposed L-shaped antenna (Figure 1) was constructed on a Rogers 5880 substrate, with $\epsilon_r = 2.2$ permittivity, thickness of 1.57 mm, and loss tangent = 0.0009. The antenna measured 28 mm × 21 mm in dimensions. The microstrip patch was two perpendicular lines forming an inverted L-shape to produce the main radiator. The proposed main radiator was designed as a simple microstrip strip line patch, which was directly linked to the port feeding. It was followed by a perpendicular line that formed an L-shape, which was modified and optimized within several steps to find the optimal band of interest at 2.4 GHz, as demonstrated in Figure 1. The proposed antenna's impedance was 51 ohms, whereas the feed line was linked to matching a 50-ohm impedance. In order to find the impedance-matching bandwidth, a rectangular slot was also created in the ground plane's middle section, not far from the feed line. Using parametric study for various values, the impact of the L shape and ground slot was clarified. The proposed antenna was created and measured to confirm its validity. Figure 2 shows the fabricated antenna.

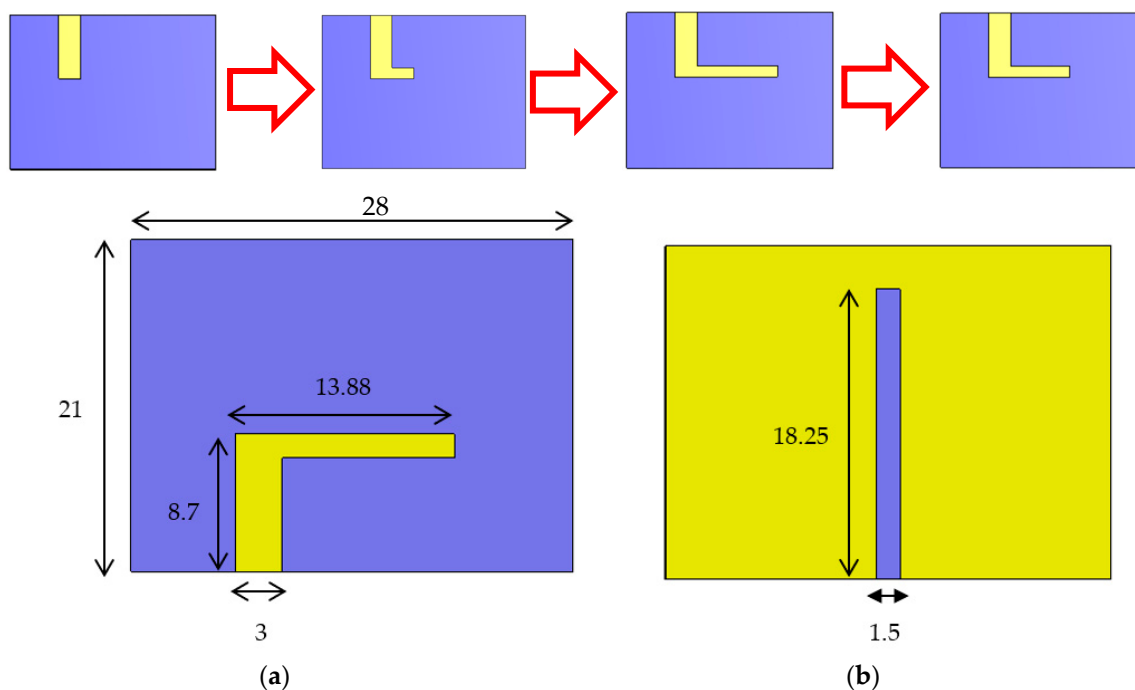


Figure 1. Antenna topology: (a) front patch, (b) back side ground plane. Unit: mm.

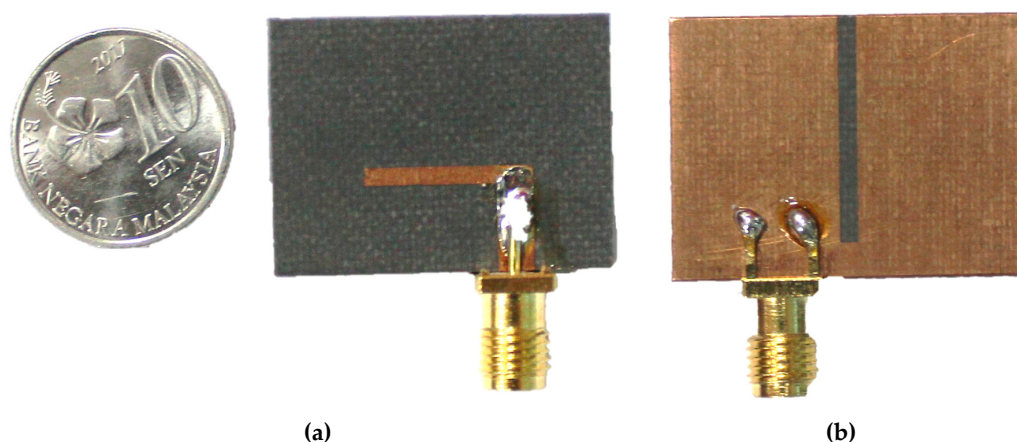


Figure 2. Fabricated prototype: (a) patch, (b) backside ground.

3. Parametric Study Working Principles

The structure's key parameters are illustrated in later parts to show how they affect its functionality. The proposed antenna performance depends mainly on the dimensions of the L-shaped strip, as well as the height and width of the aperture at the ground plane.

3.1. Working Principles

The simulated current distribution is examined and studied in order to shed light on the characteristics and operating principles of the proposed antenna. Figure 3a displays the antenna's current distribution at 2.4 GHz. The radiating element of the proposed antenna demonstrates that the principal radiator is the region of the external edges of the L radiating element, where the majority of the current distribution is focused. However, the patch's high current distribution on the upper side of the L shape helps the antenna's resonance through shifting it at 2.4 GHz, while the antenna's expanded top portion of the L shape has an impact on its gain due to the appearance of the extraordinary current on the upper part.

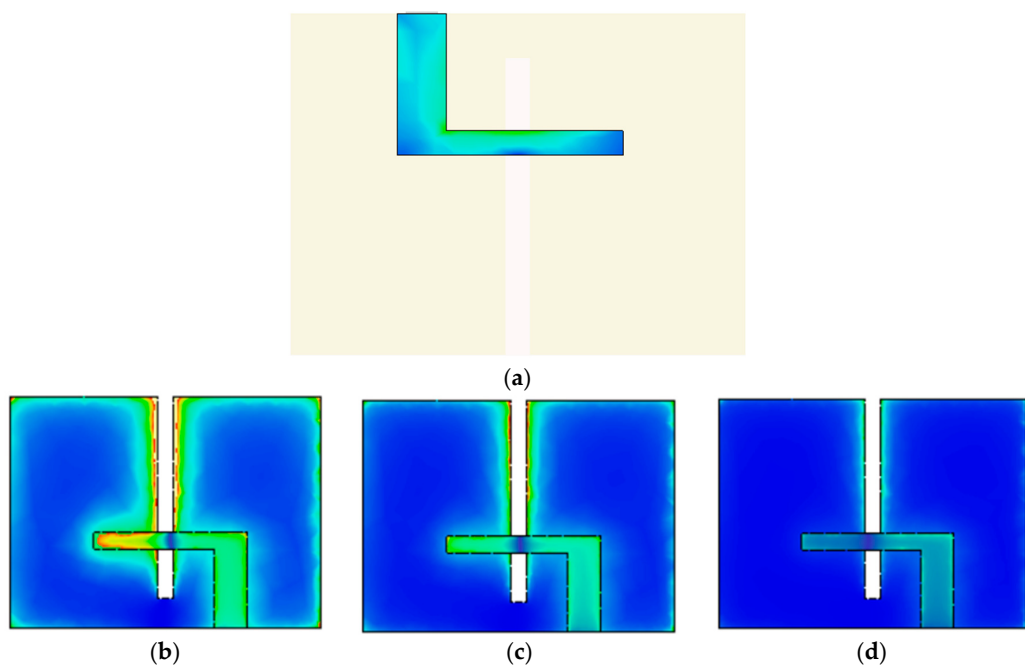


Figure 3. Simulated of optimized antenna current distribution at frequency (a) 2.4 GHz (b) 2.44 GHz; (c) 2.48 GHz; (d) 2.58 GHz.

Figure 3b displays the surface current distribution in the upper antenna arm at the resonant frequency of 2.44 GHz, whereas the whole structure exhibits single-order resonance properties. The L shape with a backside slot cut in the ground perturbs the current distribution, creating resonance at 2.4 GHz. However, the antenna's operation in the slightly shifted frequencies of 2.48 GHz and 2.58 GHz can be attributed to two distinct minima, which are seen for the current for both cases: one at the end of the arm and the other at several points in the upper edge. In contrast, low current concentration via the L shape is achieved in the case of non-resonating bands, as seen in Figure 3c,d.

3.2. Aperture's Length (L) and Width (W)

The aperture slot length (L) and width (W) affect the resonance frequency bandwidth significantly, as illustrated in Figure 4.

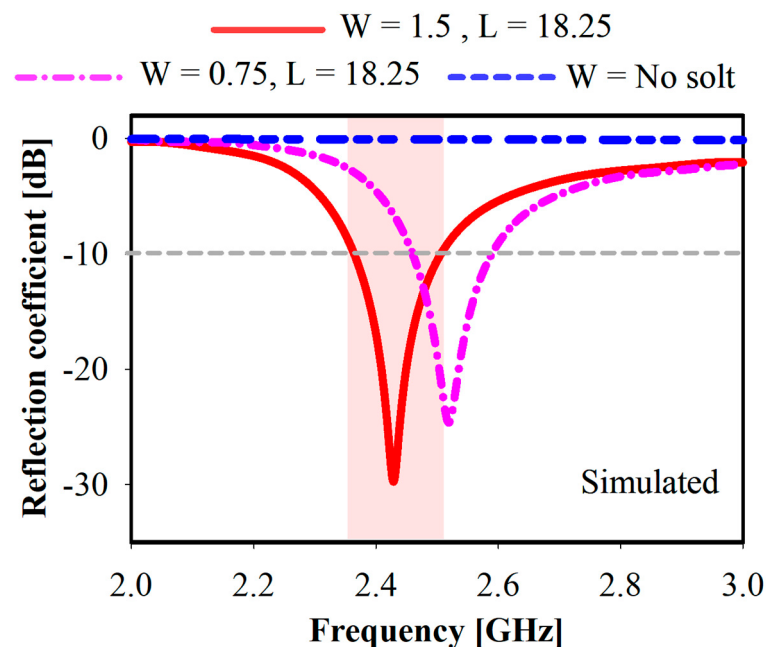


Figure 4. Simulated reflection coefficients for different antenna lengths (L).

Narrower W with 0.75 mm shifts the bandwidth towards a higher frequency. Both L and W are varied together, whereas the resonance at 2.4 GHz totally disappears in the case of no slot. However, slot $L = 18.25$ mm and $W = 1.5$ mm are the optimal dimensions for the achieved bandwidth.

3.3. Patch's Length (LP) and Width (WP)

It is observed that the increment of the patch's line length (LP) leads to enlarged bandwidths at 2.4 GHz. Figure 5 demonstrates the simulated reflection coefficient of the proposed antenna. LP is kept above -10 dB in the case of sort LP at 8 mm, whereas the resonance at 2.4 GHz starts to disappear. Furthermore, no resonance can be seen when $LP = 3$ mm. The optimum value for the LP is 18.25, which is chosen to attain the targeted operating frequency band. However, a very narrow bandwidth is observed when the patch's width $WP = 1$ mm and the length remains constant at 18.25 mm, as illustrated in Figure 6. This resonance will be continuously reduced if the WP decreases accordingly.

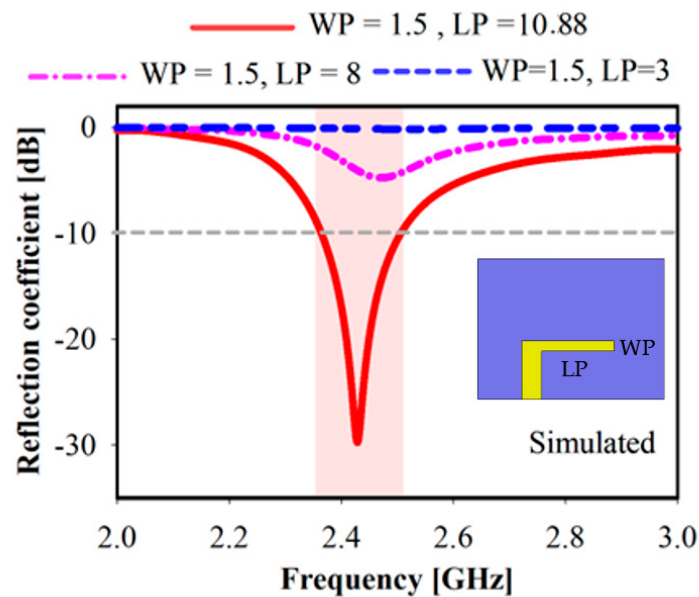


Figure 5. Simulated different patch's length reflection coefficient.

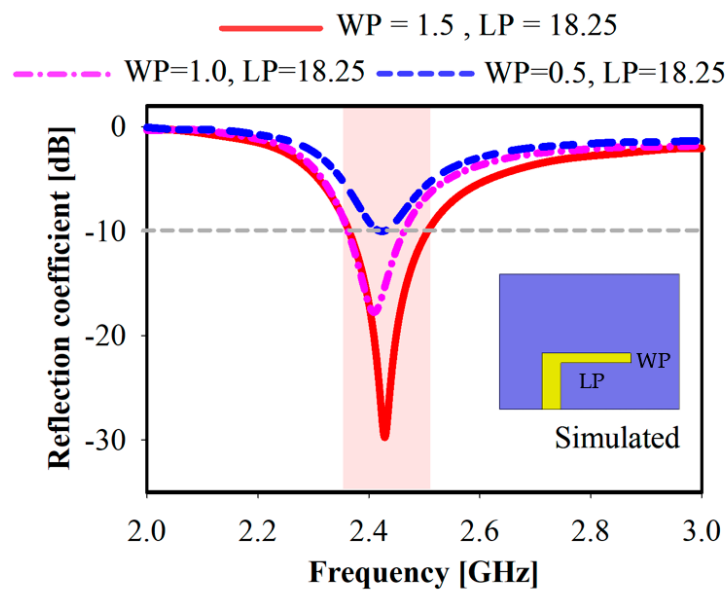


Figure 6. Simulated different patch widths reflection coefficient.

4. Results and Discussion

To ensure the greatest performance in terms of the band of interest, bandwidth, compact size, and gain, a number of crucial characteristics of the proposed L-shaped antenna were optimized prior to the choice and manufacture of the final structure. The simulation and measurement of the final prototype's reflection coefficient are shown in Figure 7. The antenna's final optimized overall dimensions are 28 mm × 21 mm × 1.6 mm. The proposed antenna's realized bandwidth spans a minimum of 2.36 GHz and a maximum of 2.5 GHz (with a total of 145 MHz, i.e., 5.8%). Figure 8 illustrates the efficiency of the L-shaped antenna. The exhibited radiation and total efficiencies have peaks of 98% and 97%, respectively, at 2.4 GHz. In addition, the achieved gain of the proposed single antenna in the operation bandwidth is defined. The realized gain can reach up to 2.09 dBi, though it decreases slightly towards a lower frequency range, as demonstrated in Figure 8. The simulated and measured findings showed a good agreement. Furthermore, Figure 9 displays the achieved simulated gain with different widths of the slot placed on the ground

plane; this figure shows the effect of that slot on achieving high realized gain on the 1.5 mm width.

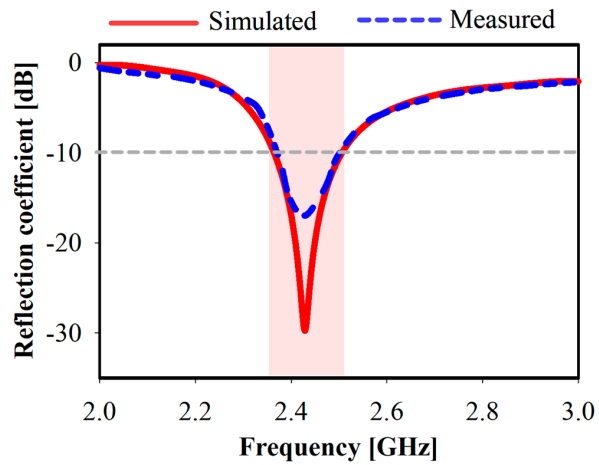


Figure 7. Simulated and measured reflection coefficient.

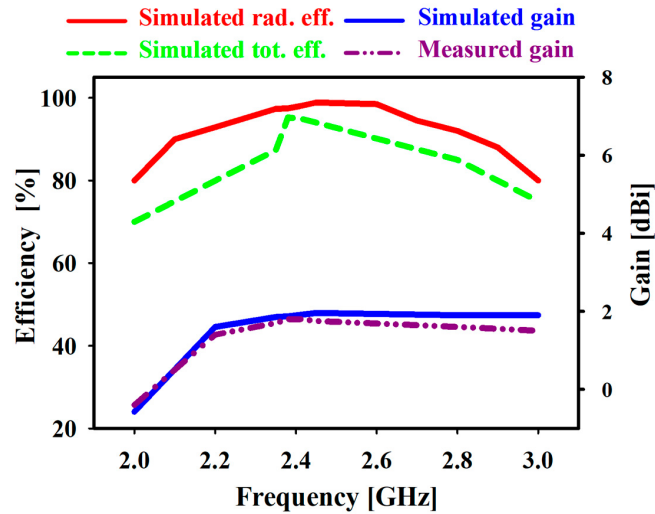


Figure 8. Simulated and measured gain, radiation efficiency, and total efficiency for proposed antenna.

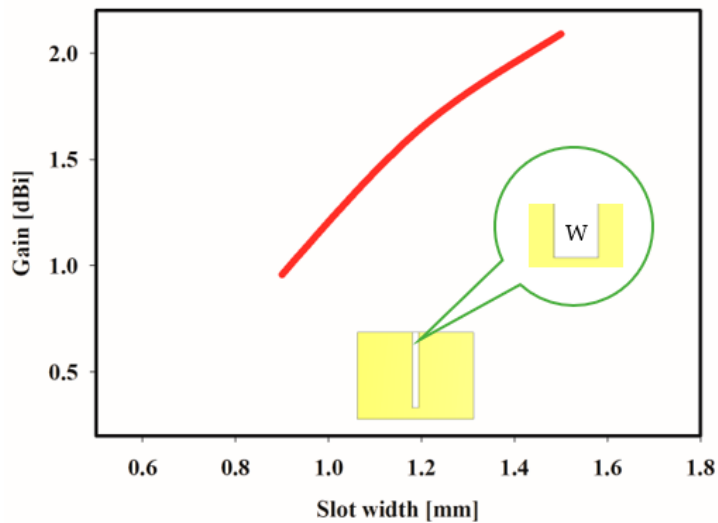


Figure 9. Simulated analysis of gain.

Figure 10 displays the simulated and measured 2.4 GHz azimuth-plane radiation patterns. The antenna radiates in the H-plane with modest amounts of cross-polarization and vertical polarization (xz-plane). The proposed antenna has a figure-of-eight radiation pattern at 2.4 GHz in the E-plane (yz-plane). Figure 11 shows the S11 reflection coefficient and radiation pattern measurement setup for the proposed antenna.

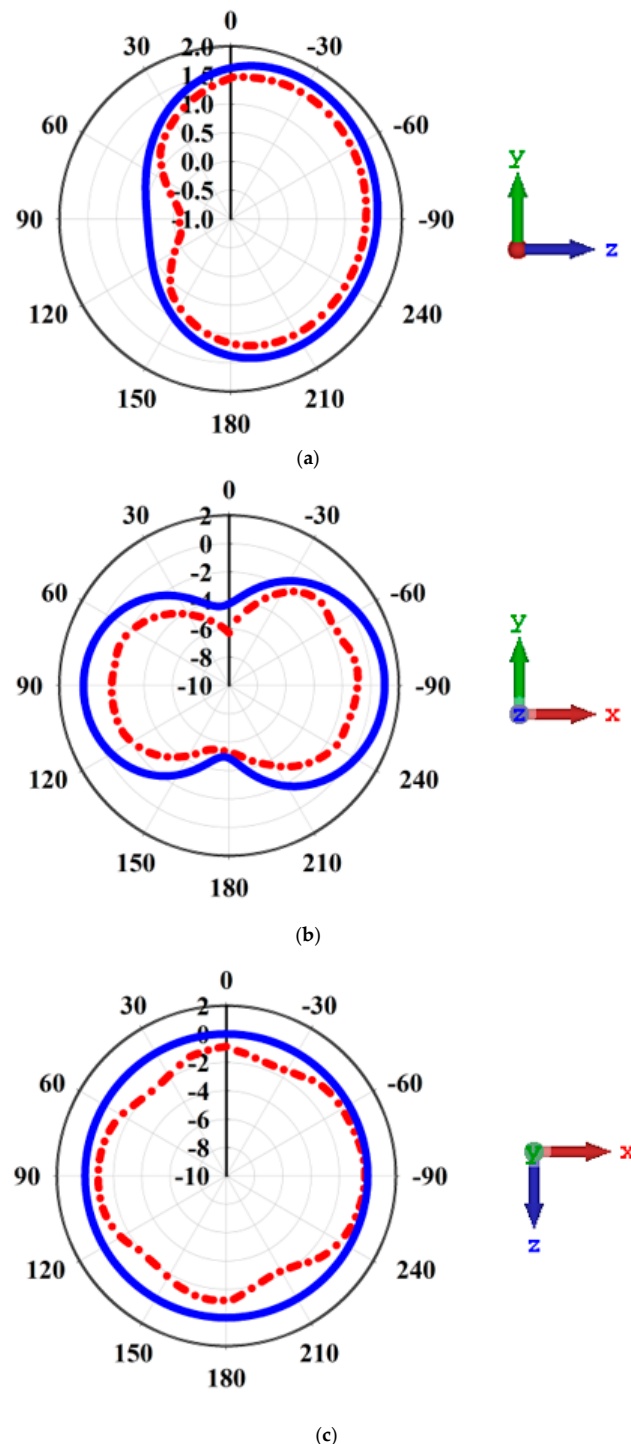


Figure 10. Two-dimensional simulated and measured radiation patterns at 2.4 GHz for planes: (a) YZ ($\phi = 90^\circ$), (b) XY ($\theta = 90^\circ$), (c) XZ ($\phi = 0^\circ$).

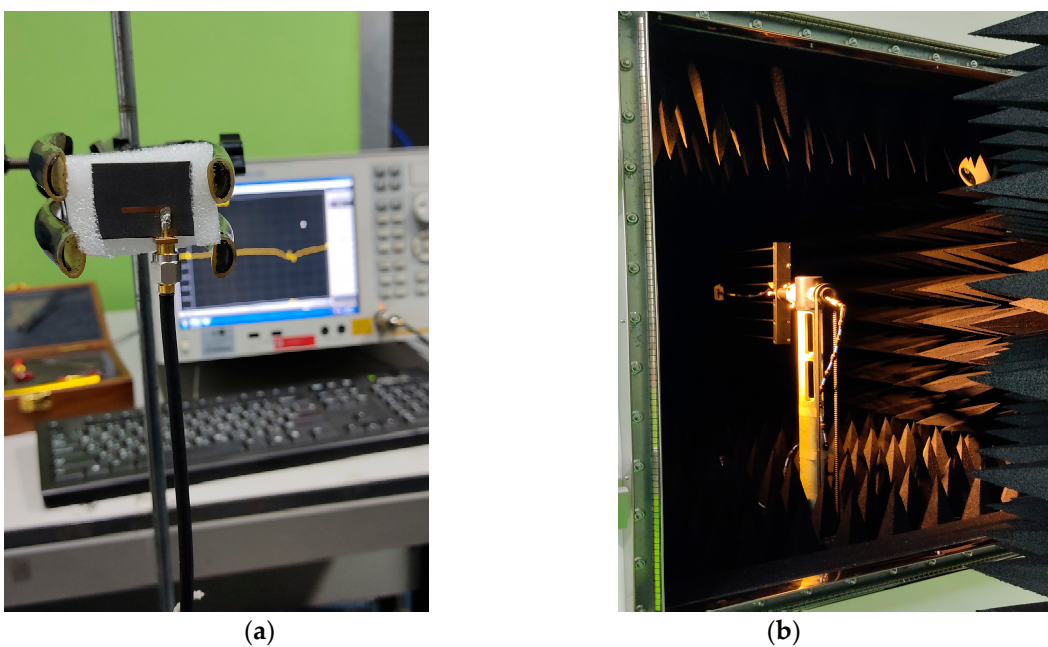


Figure 11. Measurement setup: (a) S11, (b) radiation pattern.

Figure 12 depicts the simulated face-to-face group delay (GD) of the suggested compact antenna. Over the frequency range, it is almost homogeneous with little change (1.3 ns). As a result, it is clear that there was no signal distortion between the transmitting and receiving antenna systems. Additionally, the transfer function (TF) in Figure 10 with the transmission coefficient S21 exhibits reduced distortion. As a result, this antenna is suited to use in IoT and short-range communications applications because of the realized TF and flat GD over the frequency range.

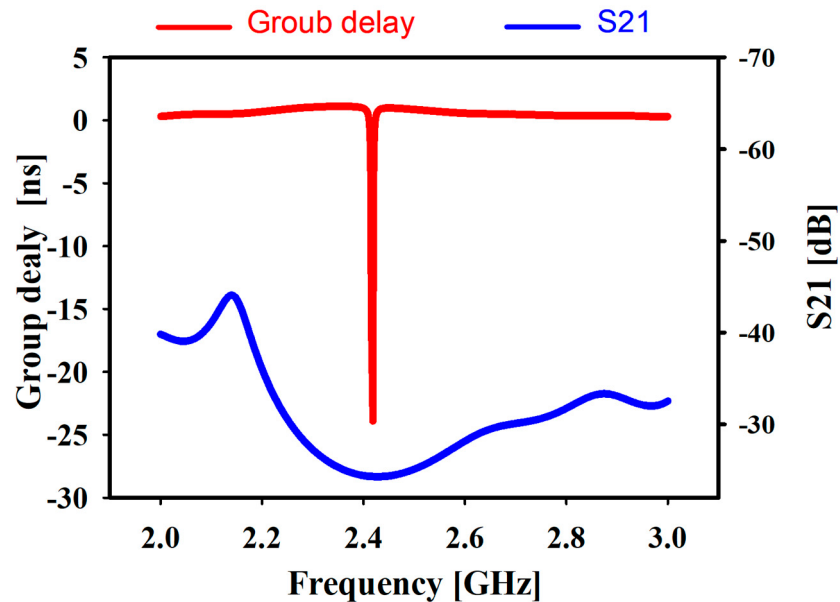


Figure 12. Face-to-face position response of group delay.

The suggested antenna is contrasted with the current microstrip antenna at 2.4 GHz in Table 1. A variety of 2.4 GHz antenna topologies were reported by researchers, together with parametric and experimental results for various applications. The comparison demonstrates that, in contrast to all of the other designs, the proposed compact antenna has a higher gain. The comparison table makes clear that existing antenna dimensions are typically

bigger than those of the suggested antenna. Furthermore, the performance of the proposed antenna at 2.4 GHz is better than others, and is a workable solution for 2.4 GHz IoT.

Table 1. Performance comparison for state of proposed L-shaped antenna at 2.4 GHz.

| Year | Ref. | Antenna Shape | Antenna Size | Fractional BW (%) | Rad. Eff. (%) | Gain (dB) | Applications |
|------|------------|----------------|---------------|-------------------|---------------|-----------|----------------------|
| 2014 | [11] | Meander line | 32.00 × 01.60 | 7.60 | - | 0.50 | * NS |
| 2017 | [34] | Spiral slot | 12.45 × 13.05 | 7.50 | - | 1.33 | * NS |
| 2018 | [35] | Uniplanar | 10.00 × 19.00 | 8.00 | - | 1.20 | 2.5 GHz applications |
| 2018 | [36] | Bowtie antenna | 29.00 × 13.70 | - | 89 | 1.47 | Wearable application |
| 2019 | [37] | Meander line | 40.00 × 10.00 | 12.5 | 79 | 1.34 | IoT |
| 2020 | [38] | Slotted SIW | 120.0 × 395.4 | 2.10 | - | 4.80 | WLAN |
| 2021 | [39] | Slot antenna | 105.0 × 85.00 | 3.20 | - | 4.00 | IoT |
| 2022 | [40] | Cage antenna | 49.00 × 49.00 | 3.20 | 93 | 3.00 | WLAN |
| 2023 | This study | L-shaped | 28.00 × 21.00 | 5.80 | 98 | 2.09 | IoT |

* NS: not specific.

5. Application Scenarios

The suggested antenna can be used for various indoor communications applications, including smart homes, airports, malls, etc. These suggested uses are viable because the proposed antenna covers the significant IoT band of microwave bands. The following subsection contains an explanation of an application scenario.

Indoor Localization Systems

Future smart homes, airports, and retail centres will use microwave and mm-wave bands for indoor connectivity to facilitate multi-system wireless communication networks, whereas microwave frequency bands will offer long-range telecommunications with average speeds that link an enormous number of multi-media gadgets and IoT devices [41]. The proposed antenna will be used to collect the received signal strength (RSS) in a specific indoor scenario within different positions of the mobile station subscriber, highly identifying its location without using a global position satellite (GPS). This technique analyzes variations in RSS between one transmitter, known as a single base station (SBS), and a huge number of subscriber mobile station receivers. Therefore, it will be evaluated based on the algorithm proposed in [42,43] to estimate the unknown mobile station receiver positions with the SBS.

6. Conclusions

Nowadays, one of the benefits of IoT applications is the use of antenna terminals as wireless sensor technologies. In this study, a prospective solution to be utilized in IoT-based applications is introduced. The proposed compact antenna is modified and constructed as an L-shaped antenna for the ISM at the 2.4 GHz frequency band. The influence of the straightforward L-shape patch, along with an etching rectangular backside slot in the ground plane, was examined numerically and verified using measurements. The obtained results showed that the antenna had an excellent radiation efficiency of 98% and simulated attained gain up to 2.09 dBi, which are well-thought-out as special considerations compared to other conventional antennas. The proposed antenna is a viable candidate for wireless fourth-generation 4G and IoT, especially in an indoor development scenario for smart offices/homes. Upcoming work will apply the proposed antenna in radio frequency (RF) modules for IoT sensors as a transmitter for indoor localization estimation using only one base station.

Author Contributions: Conceptualization, M.F.Z. and S.S.A.-B.; methodology, M.F.Z. and S.S.A.-B.; software, M.F.Z. and S.S.A.-B.; validation, M.F.Z. and S.S.A.-B.; formal analysis, M.F.Z., S.S.A.-B. and M.J.; investigation, M.F.Z. and S.S.A.-B.; resources, M.F.Z. and S.S.A.-B.; data curation, M.F.Z., S.S.A.-B., M.J. and A.H.R.; writing—original draft preparation, M.F.Z. and S.S.A.-B.; writing—review and editing, M.J., A.H.R., H.V., A.M.A. and M.H.; funding acquisition, M.F.Z. and S.S.A.-B., H.V. and A.M.A. All authors have read and agreed to the published version of the manuscript.

Funding: This work is supported by Researchers Supporting Project number (RSP2023R482), King Saud University, Riyadh, Saudi Arabia.

Institutional Review Board Statement: Not applicable.

Informed Consent Statement: Not applicable.

Data Availability Statement: Not applicable.

Conflicts of Interest: The authors declare no conflict of interest.

References

1. Abdulzahra, D.H.; Alnahwi, F.; Abdullah, A.S.; Al-Yasir, Y.I.A.; Abd-Alhameed, R.A. A Miniaturized Triple-Band Antenna Based on Square Split Ring for IoT Applications. *Electronics* **2022**, *11*, 2818. [[CrossRef](#)]
2. Ibrahim, H.H.; Singh, M.J.; Al-Bawri, S.S.; Ibrahim, S.K.; Islam, M.T.; Soliman, M.S.; Islam, M.S. Low Profile Monopole Meander Line Antenna for WLAN Applications. *Sensors* **2022**, *22*, 6180. [[CrossRef](#)] [[PubMed](#)]
3. Koga, Y.; Kai, M. A transparent double folded loop antenna for IoT applications. In Proceedings of the 2018 IEEE-APS Topical Conference on Antennas and Propagation in Wireless Communications (APWC), Cartagena, Colombia, 10–14 September 2018; pp. 762–765.
4. Jha, K.R.; Bukhari, B.; Singh, C.; Mishra, G.; Sharma, S.K. Compact Planar Multistandard MIMO Antenna for IoT Applications. *IEEE Trans. Antennas Propag.* **2018**, *66*, 3327–3336. [[CrossRef](#)]
5. Alibakhshikenari, M.; Virdee, B.S.; Ali, A.; Limiti, E. A novel monofilar-Archimedean metamaterial inspired leaky-wave antenna for scanning application for passive radar systems. *Microw. Opt. Technol. Lett.* **2018**, *60*, 2055–2060. [[CrossRef](#)]
6. Damis, H.A.; Khalid, N.; Mirzavand, R.; Chung, H.J.; Mousavi, P. Investigation of epidermal loop antennas for biotelemetry IoT applications. *IEEE Access* **2018**, *6*, 15806–15815. [[CrossRef](#)]
7. Alibakhshikenari, M.; Limiti, E.; Naser-Moghadasi, M.; Virdee, B.S.; Sadeghzadeh, R.A. A New Wideband Planar Antenna with Band-Notch Functionality at GPS, Bluetooth and WiFi Bands for Integration in Portable Wireless Systems. *AEU—Int. J. Electron. Commun.* **2017**, *72*, 79–85. [[CrossRef](#)]
8. Liu, C.; Guo, Y.-X.; Xiao, S. A Hybrid Patch/Slot Implantable Antenna for Biotelemetry Devices. *IEEE Antennas Wirel. Propag. Lett.* **2013**, *11*, 1646–1649. [[CrossRef](#)]
9. Al-Gburi, A.J.A.; Zakaria, Z.; Palandoken, M.; Ibrahim, I.M.; Althuwayb, A.A.; Ahmad, S.; Al-Bawri, S.S. Super Compact UWB Monopole Antenna for Small IoT Devices. *Comput. Mater. Contin.* **2022**, *73*, 2785–2799.
10. Al-Bawri, S.S.; Islam, M.S.; Wong, H.Y.; Jamlos, M.F.; Narbudowicz, A.; Jusoh, M.; Sabapathy, T.; Islam, M.T. Metamaterial Cell-Based Superstrate towards Bandwidth and Gain Enhancement of Quad-Band CPW-Fed Antenna for Wireless Applications. *Sensors* **2020**, *20*, 457. [[CrossRef](#)]
11. Lee, M.W.; Leung, K.; Chow, Y. Low cost meander line chip monopole antenna. *IEEE Trans. Antennas Propag.* **2013**, *62*, 442–445. [[CrossRef](#)]
12. Shabbir, T.; Islam, M.T.; Misran, N.; Al-Bawri, S.S.; Singh, S. Broadband single-layer reflectarray antenna loaded with meander-delay-lines for X-band applications. *Alex. Eng. J.* **2020**, *60*, 1105–1112. [[CrossRef](#)]
13. Kuo, J.-S.; Wong, K.-L. A compact microstrip antenna with meandering slots in the ground plane. *Microwave Opt. Technol. Lett.* **2001**, *29*, 95–97. [[CrossRef](#)]
14. Sadat, S.; Fardis, M.; Geran, F.; Dadashzadeh, G.; Hojjat, N.; Roshandel, M. A compact microstrip square-ring slot Antenna for UWB applications. In Proceedings of the 2006 IEEE Antennas and Propagation Society International Symposium, Albuquerque, NM, USA, 9–14 July 2006; pp. 4629–4632.
15. Chen, J.-H.; Yang, C.-K.; Cheng, C.-Y.; Yu, C.-C.; Hsu, C.-H. Gain enhancement of a compact 2.4-GHz meander antenna using inductive feed and capacitive load. *Microwave Opt. Technol. Lett.* **2017**, *59*, 2598–2604. [[CrossRef](#)]
16. Al-Bawri, S.S.; Hwang Goh, H.; Islam, M.S.; Wong, H.Y.; Jamlos, M.F.; Narbudowicz, A.; Jusoh, M.; Sabapathy, T.; Khan, R.; Islam, M.T. Compact Ultra-Wideband Monopole Antenna Loaded with Metamaterial. *Sensors* **2020**, *20*, 796. [[CrossRef](#)] [[PubMed](#)]
17. Al-Bawri, S.S.; Islam, M.T.; Islam, M.S.; Singh, M.J.; Alsaif, H. Massive metamaterial system-loaded MIMO antenna array for 5G base stations. *Sci. Rep.* **2022**, *12*, 14311.
18. Yildirim, B.; Cetiner, B.A. Enhanced gain patch antenna with a rectangular loop shaped parasitic radiator. *IEEE Antennas Wirel. Propag. Lett.* **2008**, *7*, 229–232. [[CrossRef](#)]
19. Cho, Y.J.; Hwang, S.H.; Park, S.O. A dual-band internal antenna with a parasitic patch for mobile handsets and the consideration of the handset case and battery. *IEEE Antennas Wirel. Propag. Lett.* **2005**, *4*, 429–432.

20. Chang, L.; Chen, L.L.; Zhang, J.Q.; Li, D. A Broadband Dipole Antenna with Parasitic Patch Loading. *IEEE Trans. Antennas Propag.* **2018**, *17*, 1717–1721. [[CrossRef](#)]
21. Liang, J.; Chiau, C.C.; Chen, X.; Parini, C.G. Study of a printed circular disc monopole antenna for UWB systems. *IEEE Trans. Antennas Propag.* **2005**, *53*, 3500–3504. [[CrossRef](#)]
22. Lin, J.-F.; Chu, Q.-X. Enhancing bandwidth of CP microstrip antenna by using parasitic patches in annular sector shapes to control electric field components. *IEEE Antennas Wirel. Propag. Lett.* **2018**, *17*, 924–927. [[CrossRef](#)]
23. Fan, S.T.; Yin, Y.Z.; Lee, B.; Hu, W.; Yang, X. Bandwidth Enhancement of a Printed Slot Antenna With a Pair of Parasitic Patches. *IEEE Antennas Wirel. Propag. Lett.* **2012**, *11*, 1230–1233. [[CrossRef](#)]
24. Arif, A.; Zubair, M.; Ali, M.; Khan, M.U.; Mehmood, M.Q. A Compact, Low-Profile Fractal Antenna for Wearable On-Body WBAN Applications. *Antennas Wirel. Propag. Lett.* **2019**, *18*, 981–985. [[CrossRef](#)]
25. Awan, W.A.; Hussain, N.; Le, T.T. Ultra-thin flexible fractal antenna for 2.45 GHz application with wideband harmonic rejection. *AEU-Int. J. Electron. Commun.* **2019**, *110*, 152851. [[CrossRef](#)]
26. Awan, W.A.; Hussain, N.; Kim, S.; Kim, N. A Frequency-Reconfigurable Filtenna for GSM, 4G-LTE, ISM, and 5G Sub-6 GHz Band Applications. *Sensors* **2022**, *22*, 5558. [[CrossRef](#)] [[PubMed](#)]
27. Kang, Z.; Lin, X.; Tang, C.; Mei, P.; Liu, W.; Fan, Y. 2.45-GHz wideband harmonic rejection rectenna for wireless power transfer. *Int. J. Microw. Wirel. Technol.* **2017**, *9*, 977–983. [[CrossRef](#)]
28. Ali, E.M.; Awan, W.A.; Naqvi, S.I.; Alzaidi, M.S.; Alzahrani, A.; Elkamchouchi, D.H.; Falcone, F.; Alharbi, T.E.A. A Low-Profile Antenna for On-Body and Off-Body Applications in the Lower and Upper ISM and WLAN Bands. *Sensors* **2023**, *23*, 709. [[CrossRef](#)] [[PubMed](#)]
29. Bayarzaya, B.; Hussain, N.; Awan, W.A.; Sufian, M.A.; Abbas, A.; Choi, D.; Lee, J.; Kim, N. A Compact MIMO Antenna with Improved Isolation for ISM, Sub-6 GHz, and WLAN Application. *Micromachines* **2022**, *13*, 1355. [[CrossRef](#)]
30. Khan, U.R.; Sheikh, J.A.; Junaid, A.; Amin, R.; Ashraf, S.; Ahmed, S. Design of a Compact Hybrid Moore’s Fractal Inspired Wearable Antenna for IoT Enabled Bio-Telemetry in Diagnostic Health Monitoring System. *IEEE Access* **2022**, *10*, 116129–116140. [[CrossRef](#)]
31. Simorangkir, R.B.V.B.; Yang, Y.; Matekovits, L.; Esselle, K.P. Dual-Band Dual-Mode Textile Antenna on PDMS Substrate for Body-Centric Communications. *IEEE Antennas Wirel. Propag. Lett.* **2016**, *16*, 677–680. [[CrossRef](#)]
32. Awan, W.A.; Ghaffar, A.; Naqvi, S.I. PDMS Based Compact Antenna for 2.45 GHz Application having Wide Band Harmonic Suppression. In Proceedings of the 2022 IEEE International Symposium on Antennas and Propagation and USNC-URSI Radio Science Meeting (AP-S/URSI), Denver, CO, USA, 10–15 July 2022; pp. 782–783.
33. Mohamadzade, B.; Simorangkir, R.B.V.B.; Hashmi, R.M.; Gharaei, R.; Lalbakhsh, A.; Shrestha, S.; Zhadobov, M.; Sauleau, R. A Conformal, Dynamic Pattern-Reconfigurable Antenna Using Conductive Textile-Polymer Composite. *IEEE Trans. Antennas Propag.* **2021**, *69*, 6175–6184. [[CrossRef](#)]
34. Liu, W.; Xu, L.; Zhan, H. Design of 2.4 GHz/5 GHz planar dual-band electrically small slot antenna based on impedance matching circuit. *AEU-Int. J. Electron. Commun.* **2018**, *83*, 322–328. [[CrossRef](#)]
35. Naidu, P.V.; Kumar, A.; Rajkumar, R. Design, analysis and fabrication of compact dual band uniplanar meandered ACS fed antenna for 2.5/5 GHz applications. *Microsyst. Technol.* **2018**, *25*, 97–104. [[CrossRef](#)]
36. Othman, N.; Samsuri, N.A.; Rahim, M.K.A.; Kamardin, K.; Majid, H.A. Meander bowtie Antenna for Wearable Application. *TELKOMNIKA* **2018**, *16*, 1522–1526. [[CrossRef](#)]
37. Islam, M.S.; Islam, M.T.; Ullah, M.A.; Beng, G.K.; Amin, N.; Misran, N. A modified meander line microstrip patch antenna with enhanced bandwidth for 2.4 GHz ISM-band Internet of Things (IoT) applications. *IEEE Access* **2019**, *7*, 127850–127861. [[CrossRef](#)]
38. Izzuddin, A.; Dewantari, A.; Setijadi, E.; Palantei, E.; Rahardjo, E.T.; Munir, A. Design of 2.4 GHz Slotted SIW Array Antenna for WLAN Application. In Proceedings of the 2020 International Conference on Radar, Antenna, Microwave, Electronics, and Telecommunications (ICRAMET), Tangerang, Indonesia, 18–20 November 2020; pp. 70–73.
39. Xu, Y.; Wen, S.; Dong, Y. Compact Slot Antenna with Extended Bandwidth Integrated on Metal Box for 2.4 GHz IoT Applications. In Proceedings of the 2021 IEEE MTT-S International Wireless Symposium (IWS), Nanjing, China, 23–26 May 2021; pp. 1–3.
40. Liu, Z.; Zhang, Y.; He, Y.; Li, Y. A Compact-Size and High-Efficiency Cage Antenna for 2.4-GHz WLAN Access Points. *IEEE Trans. Antennas Propag.* **2022**, *70*, 12317–12321. [[CrossRef](#)]
41. Hussain, N.; Kim, N. Integrated Microwave and mm-Wave MIMO Antenna Module with 360° Pattern Diversity For 5G Internet-of-Things. *IEEE Internet Things J.* **2022**, *9*, 24777–24789. [[CrossRef](#)]
42. Al-Bawri, S.S.; Islam, M.T.; Singh, M.J.; Jamlos, M.F.; Narbudowicz, A.; Ammann, M.J.; Schreurs, D.M.M.P. RSS-Based Indoor Localization System with Single Base Station. *Comput. Mater. Contin.* **2022**, *70*, 5437–5452. [[CrossRef](#)]
43. Al-Bawri, S.S.; Islam, M.S.; Sahaq, K.S.B.; Marai, M.S.; Jusoh, M.; Sabapathy, T.; Padmanathan, S.; Islam, M.T. Multilayer base station antenna at 3.5 GHz for Future 5G Indoor Systems, 2019. In Proceedings of the 2019 IEEE First International Conference of Intelligent Computing and Engineering (ICOICE), Hadhramout, Yemen, 15–16 December 2019; pp. 1–4.

Disclaimer/Publisher’s Note: The statements, opinions and data contained in all publications are solely those of the individual author(s) and contributor(s) and not of MDPI and/or the editor(s). MDPI and/or the editor(s) disclaim responsibility for any injury to people or property resulting from any ideas, methods, instructions or products referred to in the content.